Theoretical thermal performance of cross-flow finned heat pipe heat exchanger used for air conditioning in surgery rooms

Élcio Nogueira

Department of Mechanic and Energy, State University of Rio de Janeiro, Resende RJ 27537-000, Brazil;
elcionogueira@hotmail.com

ABSTRACT: The thermal efficiency of heat exchangers was applied for theoretical analysis of the thermal performance of a finned heat pipe heat exchanger (FHPHE) used as an auxiliary device to control the temperature and quality of the air conditioning in operating rooms. The theoretical analysis performed is punctual and distributed. It is divided into three aspects: analysis of the evaporator section, analysis of the condenser section, and analysis of the heat exchanger in terms of overall performance. The distributed procedure contrasts with the theoretical-experimental study, which uses the concept of thermal effectiveness (ε-NTU) for global heat exchanger analysis. The developed approach considers the number of heat pipes, the number of fins, and the flow rate variation at the inlet of the heat exchanger as fundamental parameters for determining the thermophysical quantities of interest. Theoretical values were determined for the average velocities, Nusselt numbers, thermal effectiveness, heat transfer rates, and exit temperatures. The localized theoretical-experimental comparisons are consistent, and the absolute relative error for the global heat transfer rate ranges from 0.5% to 35%.

KEYWORDS: finned heat pipe; heat exchanger; air conditioning; surgery rooms; thermal efficiency

1. Introduction

This work aims to apply the thermal efficiency method to heat exchangers to theoretically analyze temperature control systems in the surgery rooms. The developed procedure is original, punctual, and distributed, contrasting with the design that applies the effectiveness method (ε-NTU) for global heat exchanger analysis. The analysis subdivides the heat exchanger into three regions: the evaporator region (precooling), the condenser region (energy recovery), and the entire system's overall effect for determining the heat exchanger's theoretical air outlet temperature.

Sukarno et al.[1] developed an experimental heating, ventilation, and air conditioning system for the operating room for energy efficiency analysis and heat recovery using a finned heat tube heat exchanger (FHPHE). The heat pipe system, arranged in a staggered configuration, consists of three, six, and nine rows of four pipes. The fresh air inlet temperature varies from 30 °C to 45 °C. In addition to experimental analysis, the authors performed a global theoretical analysis of the heat exchanger using the thermal effectiveness method (ε-NTU). They obtained maximum effectiveness of 62.7% for an inlet temperature equal to 45 °C and a heat exchanger with nine rows, that is, 36 heat pipes. They state that the global ε-NTU method can be used to compare and analyze energy recovery in air conditioning systems and that using heat pipes improves efficiency and reduces emissions.

Hakim et al.[2] investigated the HVAC system using a U-shaped finned heat exchanger to analyze the processes of heating and cooling the air. They present efficiency, coefficient of performance, and dehumidification capacity results in one- and two-row heat pipe configurations, with eight pipes per row. They note that the two-line configuration significantly affects precooling and reheating processes more than the one-line configuration. They conclude that the U-shaped heat pipe is a solution for HVAC systems that require air cooling and subsequent heating.

Putra et al.[3] conducted an experimental study with finned heat pipes to investigate heat recovery performance from the exhaust air in an ambient room. The system consists of heat pipes staggered in six lines, with external diameters equal to 13 mm and a length of 700 mm, and water as the working fluid. They analyze the inlet temperature effects, the influence of the number of heat pipelines, and the air inlet velocity. They found that the higher the air temperature at the inlet, the greater the performance of the HPHE, that is, the greater the cooling capacity of the system. Furthermore, economic analysis of system performance showed that energy consumption decreases by 0.6–4.1 GJ/year for eight h/day and 365 days/year of operation.

Barrak[4] reports that energy consumption in tropical countries should increase at a higher rate than in other countries and that energy recovery is one of the alternatives to improve thermal performance. He claims that air conditioning units and the electrical cost to run them account for half the value of energy bills and that energy recovery systems can lower this high cost. He states that heat pipes working as heat exchangers are an excellent alternative for energy recovery and that, in addition, their use can improve the quality of fresh air by decreasing the relative humidity of the air by 10%. It describes heat pipes as very efficient passive elements for heat transfer with minimal temperature differences and no need for pumping. He classifies heat pipes partially filled by the working fluid into traditional (HP), thermosyphon, and oscillating (OHP). However, he reports that the heat and mass transfer mechanisms in oscillating heat pipes (OHP) operation are partially misunderstood.

Stewart et al.[5] developed a refrigeration system emphasizing the details of the finned tube condenser using an optimization algorithm focused on efficiency. The research found that the optimization process makes it possible to determine an ideal condenser with the same performance as a traditional system, which has a cost of 23% higher. Furthermore, the optimized capacitor is demonstrated to satisfy the minimum entropy generation condition.

Nogueira[6] develops a theoretical model for determining the thermal and hydraulic performance of externally finned shell and tube heat exchangers (SFTHE) used in machine oil cooling, including non-spherical nanoparticles in the form of a cylinder. The main parameter used in the optimization process is the number of finned tubes, and the second most important is the number of heat exchanger units connected through clamps. Six finned tubes have cost-effective thermal and hydrodynamic performance despite the high viscous dissipation caused by oil in the annular region. In addition, it was demonstrated that including nanoparticles improves thermal performance, with a slight decrease in the thermodynamic Bejan number.

Górecki et al.[7] present a theoretical-experimental study of a finned heat pipe heat exchanger for small air conditioning systems. The heat exchanger uses R4044 as it is the best working fluid. The staggered arrangement of heat pipes in 20 rows has an effectiveness of 60%. The optimization process determined the configuration to minimize pressure loss. The theoretical-experimental comparison showed a level of agreement of 10%. They conclude that heat pipes with individual fins are an alternative to the heat exchanger of conventional heat pipes. Heat pipes with individual fins withstand more

significant pressure differential and are less susceptible to deformation than solid fins; they allow substitution and make cleaning easier.

Jouhara et al.[8] present a comprehensive review of heat pipes: potential applications, construction materials, and available heat pipes' performance. It subdivides the analysis directed to heat pipes into three topics: low-temperature applications, high-temperature applications, and modeling applied to heat pipes. The applications discussed in the article focus on solar, nanoparticles, thermoelectric modules, and other relevant applications. The modeling analysis includes non-Newtonian fluids, nanofluids, and automotive and nuclear systems. Finally, they discuss the limitations of heat pipes and the future perspectives related to their application.

Jouhara et al.[9] conducted theoretical-experimental work to analyze the thermal performance of a multi-pass heat pipe heat exchanger. The objective is to heat water through hot gas (air). They explore the effect of the Reynolds number changing the number of passes by incorporating deflectors and variations in the water flow rate. Experimentally, they found a significant influence of the Reynolds number on the performance of the heat exchanger. They predict the global implementation of the heat exchanger through two basic theoretical models: Log Mean Temperature Difference (LMTD) and Effectiveness Method (ε-NTU). Finally, they report the importance of heat exchangers in recovering residual energy.

2. Methodology

The system under analysis has three sets of heat pipes with 12 pipes each. Each group consists of three rows with four tubes in each row, as shown in **Figure 1a,c**, reported in reference[1]. The heated fresh air enters the pipes where the evaporation section of the heat pipes, called precooling, and a conventional heat exchanger used to keep the operating room air at a temperature between 20 °C and 25 °C are located. The air is sucked from the room through a duct system where the condenser is located, called energy recovery, as shown in **Figure 1b**. Fresh air entering the operating room must not be contaminated with any toxic elements and must be changed at a frequency of 20 to 25 times per hour. The fresh air inlet temperature varies between 30 °C and 45 °C, with a flow rate running between 0.050 kg/s and 0.095 kg/s. The saturation temperature of the working fluid is not specified. Even so, the experimental values presented by the work used as a reference must be lower than 28 °C and higher than 26 °C. For numerical simulation, we used the value of 27 °C. The number of fins used in the evaporator and condenser sections was also not explained. However, the spacing between fins is experimentally defined as 2.0 mm, leading to excessive fins in the evaporator and condenser. The number of fins on the evaporator corresponds to 77 fins, and on the condenser, 96 fins. The theoretical numerical results obtained for these numbers of fins demonstrate an over-dimensioning of the heat exchanger. Despite the increase in thermal performance, it is essential to emphasize that many fins significantly affect viscous dissipation, making the heat exchanger design unfeasible in terms of cost-effectiveness. The thermophysical properties of the air and the working fluid (water) are determined through Equations (2)–(24). The physical quantities relevant to obtaining numerical results are described through Equations (25)–(32).
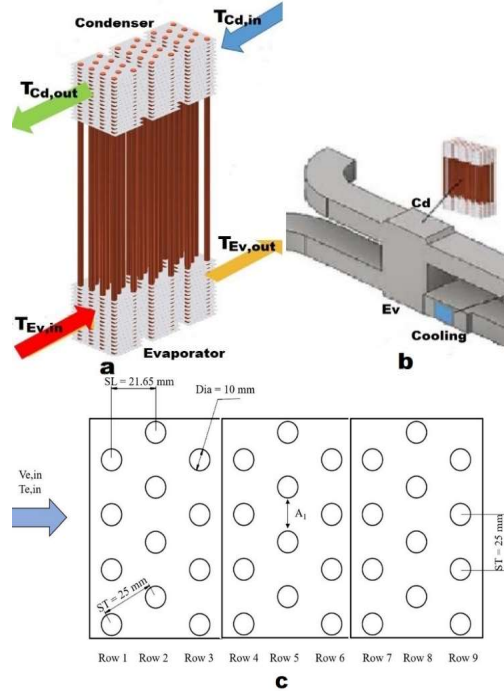
Figure 1. (a) represents the set of finned heat pipes[1]; **(b)** represents the evaporator (precooling), conventional cooling, condenser (energy recovery), and air circulation pipes[1]; **(c)** schematically represents the set of finned heat pipes arranged in the heat exchanger shell[1].

$$T_{sat} = 27.0 \ °C \ fixed \tag{1}$$

Equation (1) represents the saturation temperature of the working fluid (water) in the heat pipe.

The properties of the air, dependent on the inlet temperature $Tair_{in}$, can be obtained by the following Equations (1)–(5):

$$k_{air} = 6.91744186 \ 10^{-5}Tair_{in} + 0.02462173663 \tag{2}$$

$$\mu_{air} = 1.95483621 \ 10^{-5} + 2.735058039 \ 10^{-9}Tair_{in} + 2.309587479 \ 10^{-10} \\ Tair_{in}^2 - 4.505882353 \ 10^{-13}Tair_{in}^3 \tag{3}$$

$$Cp_{air} = 1003.728948 + 0.06727399886 * Tair_{in} + 3.565918367 \ 10^{-6} \\ Tair_{in}^2 + 8.222222222 \ 10^{-7}Tair_{in}^3 \tag{4}$$

$$\rho_{air} = 1.219135515 - 0.002152770329Tair_{in} - 3.64047479 \ 10^{-7}Tair_{in}^2 \\ +1.705882353 \ 10^{-9}Tair_{in}^3 \tag{5}$$

Equation (2) is represented by thermal conductivity. The dynamic, absolute viscosity of air characterizes Equation (3). The specific heat of air represents Equation (4). The density of air represents Equation (5).

$$v_{air} = \frac{\mu_{air}}{\rho_{air}} \tag{6}$$

$$\alpha_{air} = \frac{k_{air}}{\rho_{air}Cp_{air}} \tag{7}$$

$$Pr_{air} = \frac{v_{air}}{\alpha_{air}} \tag{8}$$

Equation (8) is represented by the Prandtl number associated with air.

The properties of the working fluid (water) can be obtained by Equations (9)–(15):

$$k_W = 0.5521904762 + 0.002561507937T_W - 1.87202381 \ 10^{-5}T_W^2 + 5.902777778 \ 10^{-8}T_W^3 \tag{9}$$

$$Cp_W = 4217.8 - 3.412833333T_W + 0.109375T_W^2 - 0.0016890625T_W^3$$
$$+ 1.34375 \ 10^{-5}T_W^4 - 4.088541667 \ 10^{-8}T_W^5 \tag{10}$$

$$\rho_W = 1002.676071 - 0.06559821429T_W - 0.003582589286T_W^2 \tag{11}$$

$$v_W = 1.787666667 \ 10^{-6} - 5.532222222 \ 10^{-8}T_W + 9.827083333 \ 10^{-10}T_W^2$$
$$- 8.965277778 \ 10^{-12}T_W^3 + 3.177083333 \ 10^{-14}T_W^4 \tag{12}$$

$$\mu_W = \rho_W v_W \tag{13}$$

$$\alpha_W = \frac{k_W}{\rho_W Cp_W} \tag{14}$$

$$Pr_W = \frac{v_W}{\alpha_W} \tag{15}$$

The saturation pressure of the working fluid (water) can be obtained through Equation (16):

$$P_{sat} = 216.7691429 - 5.927342857T_{sat} + 0.04774285714T_{sat}^2 \tag{16}$$

The properties of saturated steam are obtained through the Equations (17)–(23):

$$v_l = 0.001585485714 - 1.831904762 \ 10^{-5}T_{sat} + 1.957142857 \ 10^{-7}$$
$$T_{sat}^2 - 6.666666667 \ 10^{-10}T_{sat}^3 \tag{17}$$

$$\rho_l = \frac{1}{v_l} \tag{18}$$

$$v_V = 21.45466571 - 0.3398517143T_{SAT} + 0.001419714286T_{sat}^2 \tag{19}$$

$$\rho_v = \frac{1}{v_v} \tag{20}$$

$$h_l = 2.184 + 4.2124T_{sat} \tag{21}$$

$$h_v = 1.540666667T_{sat} + 2521.596667 \tag{22}$$

$$h_{lv} = h_v - h_l \tag{23}$$

h_{lv} is the latent heat of vaporization.

Equation (24), represented by σ_{Water} and reported by Putra et al.[3], is the surface tension for water:

$$\sigma_{Water} = 0.07275d0\big(1 - 0.002d0(K - 291)\big) \tag{24}$$

where K is saturation temperature in Kelvin.

$$C_{sf} = 0.006 \tag{25}$$

The assumed constant for the surface-fluid combination represents Equation (25). The value 0.006 originally presented by Rhosenow, valid for the copper-water pair, is reported by Jouhara et al.[9].

$$NHP = 12 \ default; 12 \le NHP \le 36 \tag{26}$$

$$N_{Fin} = 22 \ default; \quad 0 \le N_{Fin} \le 30 \tag{27}$$

$$NHP_{byrows} = 4 \tag{28}$$

$$Nrows = \frac{NHP}{NHP_{byrows}}, \quad 3 \le Nrows \le 9 \tag{29}$$

The total number of heat pipes in the heat exchanger represents Equation (26). The number of fins $NFin$ considered in the evaporator or condenser is defined by Equation (27). The number of heat pipes per row NHP_{byrows} is defined by Equation (28).

$$Vair_{inlet} = 1.5 \ m/s \ default; \quad 1.5 \le Vair_{inlet} \le 2.5 \tag{30}$$

$$0.050 \leq \dot{m}_{air} \leq 0.095 \tag{31}$$

The experimental value of the air velocity at the inlet of the heat exchanger $Vair_{inlet}$ is defined by Equation (30). The mass flow rate of air at the inlet of the heat exchanger $\dot{m}_{air}$ is defined by Equation (31).

The distributed analytical approach is subdivided into the evaporator, the condenser, and the global FHPHE.

2.1. The evaporator section of the heat pipe

In the specific case under analysis, the evaporator region is called precooling of the heated fresh air, which enters the pipe before passing through a conventional cooling system. The inlet temperature of heated fresh air varies between 30 °C and 45 °C. The cooled air enters the operating room at a temperature that varies from 20 °C minimum to 25 °C maximum. The air inside the room is changed with a frequency of 20 to 25 times per hour. For this to happen, it passes through the exhaust pipe where the energy recovery system is located, that is, the condensation region of the working fluid of the heat pipe. The inlet flow rate of fresh, heated air in the evaporator region varies between 0.050 kg/s and 0.095 kg/s.

$$\dot{m}_{air} = 0.050 \ kg/s \ defaut \tag{32}$$

The formulation used to simulate the heat exchange process in the evaporator is established through Equations (33)–(72).

$$TEv_{in} = 30.0 \ °C \ default; \quad 30.0 °C \leq TE_{in} \leq 45.0 °C \tag{33}$$

The fresh air inlet temperature in the evaporator region, defined by Equation (33), is represented by TEv_{in}.

$$h_{boil} = \mu_l h_{lv} \left(\frac{g(\rho_l - \rho_v)}{\sigma_{water}} \right)^{1/2} \left(\frac{Cp_l}{C_{sf} h_{lv} Pr_l} \right)^3 \Delta T_{sat}^2 \tag{34}$$

The estimated heat transfer coefficient for the boiling process, initially presented by Rohsenow[10] and related by Jouhara et al.[9], is given by Equation (34), represented by h_{boil}.

$$\Delta T_{Evsat} = TEv_{in} - T_{sat} \tag{35}$$

$$D_{ext} = 10.3 \ 10^{-3} \ m \tag{36}$$

$$D_{int} = 10.0 \ 10^{-3} \ m \tag{37}$$

The outside and inside diameters of the heat pipe are represented by D_{ext} and D_{int} are given by Equations (36) and (37).

$$kW = 380.0 \tag{38}$$

The thermal conductivity of the heat pipe material (Copper), represented by Equation (38), is given by kW.

$$LEv = 160.0 \ 10^{-3} \tag{39}$$

$$LEv_H = N_{Rows} \frac{LEv}{9.0} \tag{40}$$

LEv Equation (39) illustrates the length of the heat pipe evaporation section and LEv_H, represented by Equation (40), is the shell's width in the evaporator region. Note that it depends on the number of heat pipes and, by hypothesis, is equal to the height of the evaporator section under analysis for nine rows of tubes.

$$t_{Fin} = 0.105 \ 10^{-3} \tag{41}$$

$$k_{Fin} = 180.0 \tag{42}$$

The thermal conductivity of the fin material (aluminium), represented by Equation (42), is given by k_{Fin}.

$$Sp_{Fin} = 7.4\ 10^{-3}\ by\ definition;\ N_{Fin} = \frac{Lev + Sp_{Fin}}{Sp_{Fin} + t_{Fin}} \tag{43}$$

Equation (43) defines the space between fins used in the theoretical model, through which the number of fins for the evaporator can be obtained.

$$C1 = 0.36;\ C2 = 0.84\ for\ NHP = 12; C2 = 0.94\ for\ NHP = 24; C2 = 0.96\ for\ NHP = 36 \tag{44}$$

The thickness of a fin, represented by Equation (41), is given by t_{Fin}. The space between fins, defined through Equation (43), is provided by Sp_{Fin}. $C1$ and $C2$ are adjustment constants to experimental results[1].

$$Dh_{EV} = \frac{4LEv_H LEv}{2(LEv_H + LEv)} \tag{45}$$

$$Re_{Ev} = \frac{4\dot{m}_{air}}{\pi Dh_{Ev}\mu_{air}} \tag{46}$$

The hydraulic diameter of the heat exchanger in the evaporator region is given by Dh_{Ev} Equation (45). The Reynolds number associated with air, represented by Equation (46), is provided by Re_{Ev}.

$$A\sec_{Ev} = \frac{\dot{m}_{air}Dh_{Ev}}{Re_{air}\,\mu_{air}} \tag{47}$$

Equation (41), represented by $A\sec_{Ev}$, is the effective area occupied by the air in the evaporator.

$$V_{Ev} = \frac{\dot{m}_{air}}{A\sec_{Ev}\rho_{air}} \tag{48}$$

The air velocity in the evaporator, V_{Ev}, is represented by Equation (48).

$$ST = 25.0 10^{-3} \tag{49}$$

$$SL = 21.65 10^{-3} \tag{50}$$

The geometric parameters ST and SL of the heat exchanger (**Figure 1**) are defined through Equations (49) and (50).

$$Vair_{\max} = \frac{ST}{SL - Dext}Vair_{inlet} \tag{51}$$

The maximum experimental speed associated with the heat exchanger, $Vair_{max}$, is represented by Equation (51).

$$Atr_{EvFin} = NFinLEv_H LEv \tag{52}$$

$$Atr_{EvHP} = NHP\pi D_{ext}(LEv - NFinSp_{Fin}) \tag{53}$$

$$A_{EvTotal} = Atr_{EvFin} + Atr_{EvHP} \tag{54}$$

The effective heat transfer area in the evaporator $AEvtr_{HP}$, associated with heat pipes, is established by Equation (53). The effective heat transfer area associated with the fin system, Atr_{EvFin}, and the total heat transfer area, $A_{EvTotal}$, are represented by Equations (52) and (54).

$$Nu_{Ev} = C1C2\,0.71 Re_{Ev}^{0.5}\,Pr_{Ev}^{0.36}(\frac{Pr_{Evair}}{Pr_{EvSurf}})^{0.25} \tag{55}$$

The Nusselt number for the air, as reported by Jouhara et al.[9], Nu_{Ev} is represented by Equation (55). Pr_{EvSurf} it is the Prandtl number on the surface of the heat pipe.

$$h_{Ev} = \frac{Nu_{Ev}k_{air}}{Dh_{EV}} \tag{56}$$

The convection heat transfer coefficient associated with air in the evaporator, Equation (56), is given by h_{Ev}.

$$mL_{EvFin} = \sqrt{\frac{2h_{Ev}}{k_{Fin}t_{Fin}}}\, LEv_H \tag{57}$$

$$\eta_{EvFin} = \frac{\text{Tanh}(mL_{EvFin})}{mL_{EvFin}} \tag{58}$$

The fin efficiency for the evaporator section is defined through Equation (58) by η_{EvFin}[6].

$$\beta_{Ev} = \frac{Atr_{EvFin}}{A_{Total}} \tag{59}$$

$$\eta'_{EvFin} = \beta_{Ev}\eta_{EvFin} + (1 - \beta_{Ev}) \tag{60}$$

The efficiency associated with the set of fins in the evaporator, weighted by the area of change of the fins η'_{EvFin}, is represented through Equation (60).

$$Uo_{Ev} = \frac{1}{\dfrac{1}{h_{boil}} + \dfrac{D_{ext} - D_{int}}{kW} + \dfrac{1}{\eta'_{EvFin}h_{Evair}}} \tag{61}$$

The global heat transfer coefficient associated with air in the evaporator, Uo_{air}, is given by Equation (61).

$$C_{Air} = \dot{m}_{air}Cp_{air} \tag{62}$$

The heat capacity of the air in the evaporator, C_{Air}, is given by Equation (62).

$$C_{Ev} = C_{air} \tag{63}$$

$$NTU_{Ev} = \frac{Uo_{Ev}A_{EvTotal}}{CEv} \tag{64}$$

The number of thermal units associated with air in the evaporator, NTU_{Ev}, is given by Equation (64).

$$Fa = \frac{NTU\sqrt{1 + C^{*2}}}{2} \; for \; cross-flow \tag{65}$$

The dimensionless number, called "fin analogy", Fa is represented by Equation (65), as defined by Fakheri[11] and reported by Nogueira and other researchers[6,11,12].

$$\eta_T = \frac{tanh(Fa)}{Fa} \tag{66}$$

The thermal efficiency associated with the heat exchanger is η_T[11].

$$\varepsilon_T = \frac{1}{\dfrac{1}{\eta NTU} + \dfrac{1 + C^*}{2}} \tag{67}$$

The thermal effectiveness associated with the heat exchanger is ε_T[11].

The heat exchanger's thermal efficiency depends on two fundamental parameters: NTU e $C^* = \frac{C_{min}}{C_{max}}$. For the physical conditions under analysis $C^* = 0.0$. Then[11],

$$Fa_{Ev} = \frac{NTU_{Ev}}{2} \tag{68}$$

$$\eta_{TEv} = \frac{tanh(Fa_{Ev})}{Fa_{Ev}} \tag{69}$$

$$\varepsilon_{TEv} = \frac{1}{\dfrac{1}{\eta_{TEv}NTU_{Ev}} + \dfrac{1}{2}} \tag{70}$$

$$\dot{Q}_{Ev} = \frac{C_{Ev}\Delta T_{Evsat}}{\dfrac{1}{\eta_{TEv}NTU_{Ev}} + \dfrac{1}{2}} \tag{71}$$

The heat transfer rate between the air and the heat pipe in the evaporating region $\dot{Q}_{Ev}$ is given by the Equation (71).

$$TEv_{out} = TEv_{in} - \frac{\dot{Q}_{Ev}}{C_{Ev}} \tag{72}$$

After passing through the evaporator (precooling), the outlet air temperature is represented through Equation (72).

2.2. The condenser section of the heat pipe

The operating room air conditioning is sucked through the exhaust pipes and passes through the heat pipe condenser region. The saturation temperature of the working fluid is higher than the temperature of the air conditioning, which varies between 20 °C and 25 °C. The heated air leaving the heat exchanger's energy recovery region is directed out of the operating room. The air conditioner's temperature that passes through the exhaust pipe and enters the condenser section is not uniform and has an average value of 22.5 °C. The air conditioning inlet flow in the condenser region varies between 0.050 kg/s and 0.095 kg/s.

The formulation used to simulate the heat exchange process in the condenser is established through Equations (73)–(102).

$$TCd_{in} = 20.0 \text{ °C } default; \quad 20.0°C \leq TCd_{in} \leq 25.0°C \tag{73}$$

The air temperature at the condenser inlet, TCd_{in}, is represented by Equation (73).

$$\Delta T_{Cdsat} = T_{sat} - TCd_{in} \tag{74}$$

Equation (74) represents the temperature difference between the condenser's air and the working fluid.

$$LCd = 190.0 \ 10^{-3} \ m \tag{75}$$

The length of the condenser section, LCd, is represented through Equation (75).

$$LCd_H = LEv_H \tag{76}$$

The width of the shell LCd_H where the heat pipes are installed is represented by Equation (76).

$$Sp_{Fin} = 7.4 \ 10^{-3} \ by \ definition; \quad N_{Fin} = \frac{LCd + Sp_{Fin}}{Sp_{Fin} + t_{Fin}} \tag{77}$$

Equation (77) defines the space between fins used in the theoretical model, through which the number of fins for the condenser can be obtained.

$$Dh_{Cd} = \frac{4LCd_H LCd}{2(LCd_H + LCd)} \tag{78}$$

The hydraulic diameter in the region of the capacitor, Dh_{Cd}, is represented by Equation (78).

9

$$Re_{Cd} = \frac{4\dot{m}_{air}}{\pi Dh_{Cd}\mu_{air}} \tag{79}$$

The Reynolds number of air in the condenser region, Re_{Cd}, is represented through Equation (79).

$$A\,sec_{Cd} = \frac{\dot{m}_{air}Dh_{Cd}}{Re_{Cd}\,\mu_{air}} \tag{80}$$

The airflow area in the condenser, $A\sec_{Cd}$, is given by Equation (80).

$$Atr_{CdFin} = NFinLCd_H LCd \tag{81}$$

The heat exchange area associated with the fins in the condenser, Atr_{CdFin}, is established through Equation (81).

$$Atr_{CdHP} = NHP\,\pi D_{ext}(LCd - NFin\,Sp_{Fin}) \tag{82}$$

The heat exchange area of the air with the heat pipes in the condenser, Atr_{CdHP}, is given by Equation (82).

$$A_{CdTotal} = Atr_{CdFin} + Atr_{CdHP} \tag{83}$$

$$h_{Cond} = 0.943[\frac{[\rho_l(\rho_l - \rho_v)h_{lv}gk_W^3]}{(\mu_W LCd\Delta T_{sat})}]^{1/4} \tag{84}$$

The condensation transfer coefficient in the heat pipe, h_{Cond}, is given by Equation (84), as reported in the study of Jouhara et al.[9].

$$Nu_{Cd} = C1C2\,0.71\,Re_{Cd}^{0.5}\,Pr_{Cd}^{0.36}(\frac{Pr_{Cd}}{Pr_{CdSurf}})^{0.25} \tag{85}$$

Equation (85) represents the Nusselt number in the condenser Nu_{Cd}, as reported in the study of Jouhara et al.[9].

$$h_{Cd} = \frac{Nu_{Cd}k_{air}}{Dh_{Cd}} \tag{86}$$

Equation (86) represents the convection heat exchange coefficient, h_{Cd}, between the air and the surface of the heat pipe.

$$mL_{CdFin} = \sqrt{\frac{2h_{Cd}}{k_{Fin}t_{Fin}}}LCd_H \tag{87}$$

$$\eta_{CdFin} = \frac{\text{Tanh}(mL_{CdFin})}{mL_{CdFin}} \tag{88}$$

The fin efficiency, η_{CdFin}, is determined through Equation (88)[6,11,12].

$$\beta_{Cd} = \frac{Atr_{CdFin}}{A_{CdTotal}} \tag{89}$$

$$\eta'_{CdFin} = \beta_{Cd}\eta_{CdFin} + (1 - \beta_{Cd}) \tag{90}$$

The efficiency associated with the fin system, weighted by the heat exchange area, is represented by Equation (90).

$$Uo_{Cd} = \frac{1}{\frac{1}{h_{Cond}} + \frac{D_{ext} - D_{int}}{kW} + \frac{1}{\eta'_{CdFin}h_{Cd}}} \tag{91}$$

Equation (91) represents the global heat transfer coefficient.

$$C_{Air} = \dot{m}_{air}Cp_{air} \tag{92}$$

$$C_{Cd} = C_{air} \tag{93}$$

The heat capacity of the air in the region of the condenser, C_{Cd}, is represented by Equation (93).

$$NTU_{Cd} = \frac{Uo_{Cd}A_{CdTotal}}{C_{Cd}} \tag{94}$$

Equation (94) represents the number of thermal units associated with the heat pipes in the condenser region.

$$Fa_{Cd} = \frac{NTU_{Cd}}{2} \tag{95}$$

The dimensionless parameter called "fin analogy" in the condenser region, Fa_{Cd}, is represented through Equation (95).

$$\eta_{TCd} = \frac{tanh(Fa_{Cd})}{Fa_{Cd}} \tag{96}$$

Equation (96) represents the thermal efficiency associated with the condenser[11].

$$\varepsilon_{TCd} = \frac{1}{\frac{1}{\eta_{TCd}NTU_{Cd}} + \frac{1}{2}} \tag{97}$$

Equation (97) represents the thermal effectiveness related to the condenser[11].

$$\dot{Q}_{Cd} = \frac{C_{Cd}\Delta T_{Cdsat}}{\frac{1}{\eta_{TCd}NTU_{Cd}} + \frac{1}{2}} \tag{98}$$

The rate of heat transfer between the air and the heat pipe in the region of the condenser is represented by Equation (98).

$$TCd_{out} = \frac{\dot{Q}_{Cd}}{C_{Cd}} + TCd_{in} \tag{99}$$

The air outlet temperature in the condenser, TCd_{out}, is defined through Equation (99).

2.3. Finned heat pipe crow-flow heat exchanger-FHPHE

The pre-cooling and energy recovery set to form a heat exchanger, with a fresh air inlet with a temperature above 28 °C and a cooled air outlet below 28 °C. The total heat transfer rate in the air conditioning process is equal to the sum of the heat transfer rates in the evaporator and the condenser $\dot{Q}_{Cd}$, according to Equation (100). Equation (101) represents the maximum transfer rate, $\dot{Q}_{Max}$, in the heat exchanger, which C_{min} is the smallest of the thermal capacities of the air involved in the process. Equation (102) represents the heat exchanger's effectiveness in the air conditioning process that passes through the operating room.

$$\dot{Q}_{FHPHE} = \dot{Q}_{Ev} + \dot{Q}_{Cd} \tag{100}$$

$$\dot{Q}_{Max} = C_{\min}(TEv_{in} - TCd_{out}) \tag{101}$$

$$\varepsilon_{FHPHE} = \frac{TEv_{in} - TCd_{out}}{TEv_{in} - TCd_{in}} \tag{102}$$

3. Results and discussion

3.1. The evaporator section of the heat pipe

The evaporator preheats the fresh air that enters the air conditioning system directed to the operating room. The air velocity is measured before it enters the heat exchanger shell, where the heat pipes are arranged. The experimental air inlet velocities in the heat exchanger are 1.5 m/s, 2.0 m/s, and 2.5 m/s. The velocity increases when the air enters the shell because the frontal area suffers a reduction. **Figure 2**

presents results for the velocity in the shell as a function of the airflow and the number of fins used in the evaporation tube of the refrigerant fluid. Equations (48)–(51) represent the velocities obtained through the theoretical model and those obtained through the experimental procedure. Velocity increases with the flow rate and decreases with the number of heat pipes as the shell area increases. Therefore, the velocities obtained through the developed model are compatible with experimental results.
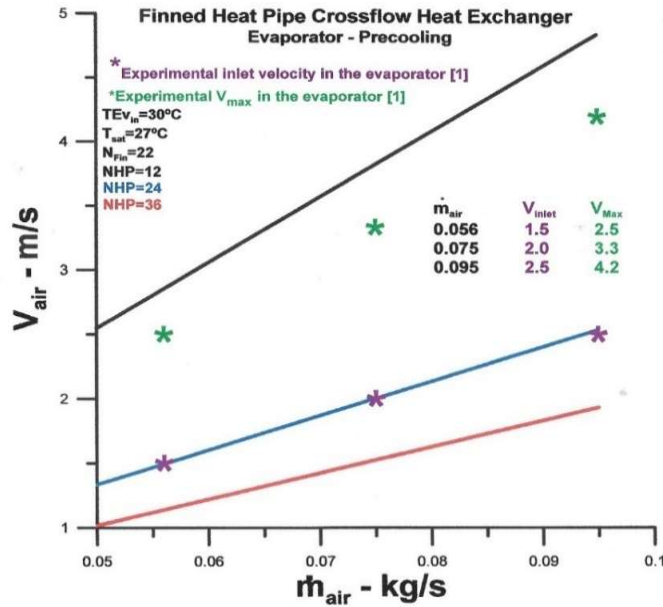

Figure 2. Air velocity versus air mass flow rate.

Figure 3 shows values for the Nusselt number in the evaporator region as a function of the airflow rate and the number of heat pipes equal to 12, 24, and 36. The Nusselt number grows as the airflow rate decreases with increasing air inlet temperature and the number of heat pipes.
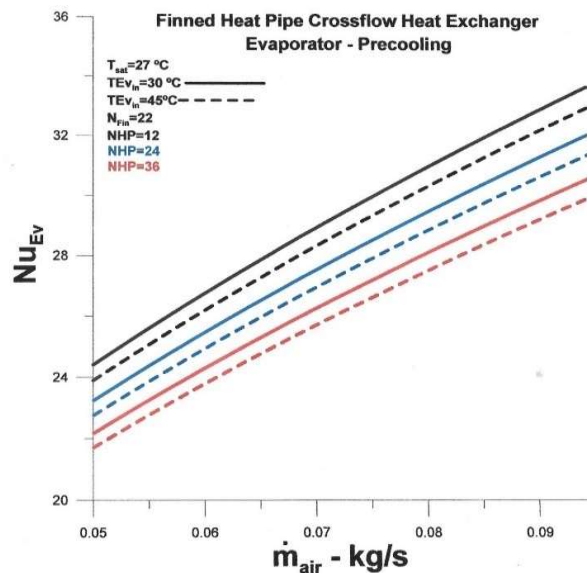

Figure 3. Nusselt number versus air mass flow rate.

Figure 4 presents results for the number of thermal units associated with the evaporator. The number of thermal units is a critical parameter in theoretical analysis using the thermal efficiency method, the effectiveness method (ε-NTU), or the logarithmic temperature difference method (LMTD). The number

of thermal units increases with the number of heat pipes, that is, with the increase in the area available for heat exchange and the increase in the difference between the air inlet temperature and the saturation temperature of the working fluid.
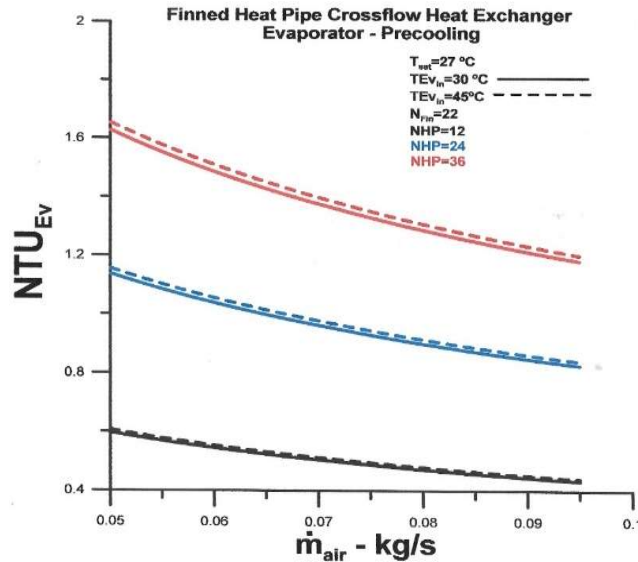

Figure 4. Number of thermal units at the evaporator versus air mass flow rate.

Figure 5 presents results for the global heat transfer coefficient, which decreases with the number of heat pipes and increases with the increase in the air inlet temperature.
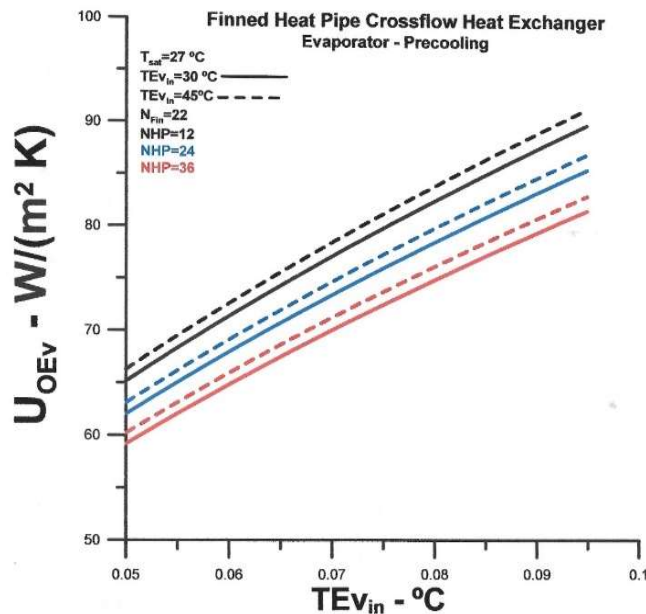

Figure 5. Global heat transfer rate coefficient at the evaporator versus air inlet temperature.

The thermal effectiveness in the evaporator region is represented in **Figure 6** as a function of the air inlet temperature, the number of heat pipes, and the airflow rate. The number of fins used in the model is equal to 22. The efficiency increases with the number of heat pipes, decreases with the airflow rate, and suffers a slight variation with the inlet temperature. The experimental values presented through reference[1] are within the range of values obtained through the theoretical model and show a significant growth trend with the number of heat pipes.
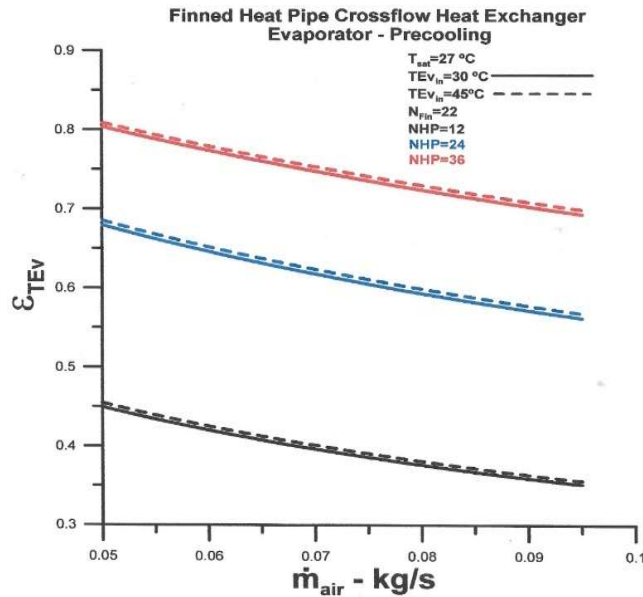
Figure 6. Effectiveness of the evaporator versus number of heat pipes and air inlet temperature.

Figure 7 shows the thermal effectiveness in the evaporator region as a function of heat pipes, airflow rate equal to 0.05 kg/s, and inlet air temperature. Effectiveness increases with the number of heat pipes and air inlet temperature. The theoretical-experimental comparison shows an absolute relative deviation between 2.5% and 22%.
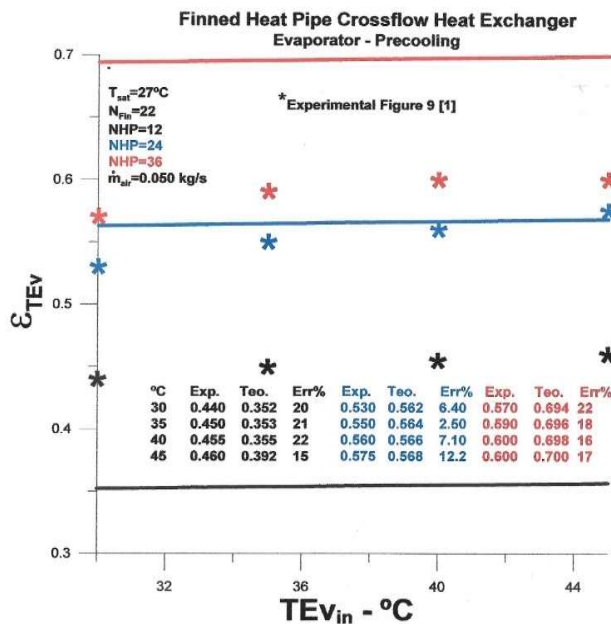

°C	Exp.	Teo.	Err%	Exp.	Teo.	Err%	Exp.	Teo.	Err%
30	0.440	0.352	20	0.530	0.562	6.40	0.570	0.694	22
35	0.450	0.353	21	0.550	0.664	2.50	0.590	0.696	18
40	0.455	0.355	22	0.560	0.566	7.10	0.600	0.698	16
45	0.460	0.392	15	0.575	0.568	12.2	0.600	0.700	17

Figure 7. Effectiveness at the evaporator versus the number of heat pipes and air inlet temperature for mass flowrate equal 0.050 kg/s.

The heat transfer rate in the evaporator is represented in **Figure 8** for heat pipes, mass flow rate, and inlet temperature. The heat transfer rate increases with the number of heat pipes and airflow rate. **Figure 8** demonstrates that the temperature of the air entering the evaporator increases the heat transfer rate since the temperature of the working fluid is constant and equal to 27 °C.
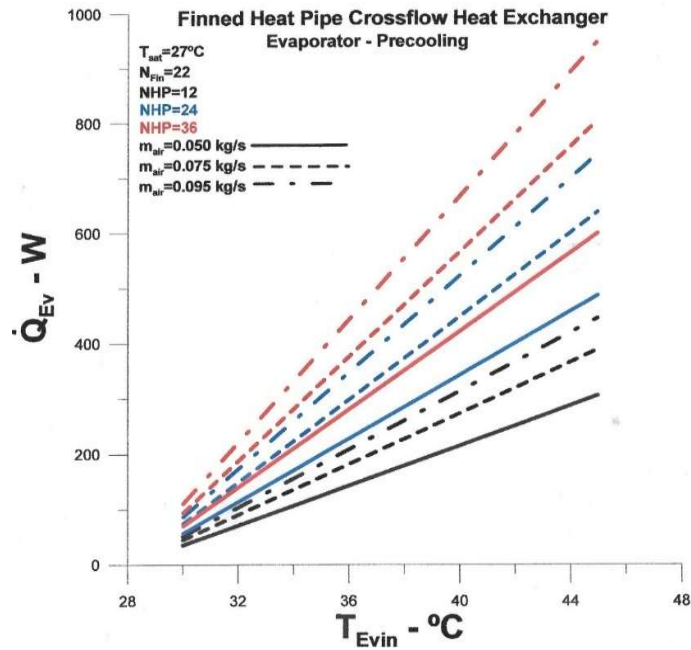
Figure 8. Heat transfer rate at the evaporator versus air mass flow rate and air inlet temperature.

Figure 9 emphasizes the influence of the number of heat pipes, the air inlet temperature, and the air inlet temperature on the heat transfer rate in the evaporator region. The heat transfer rate increases the number of heat pipes and inlet air temperature.
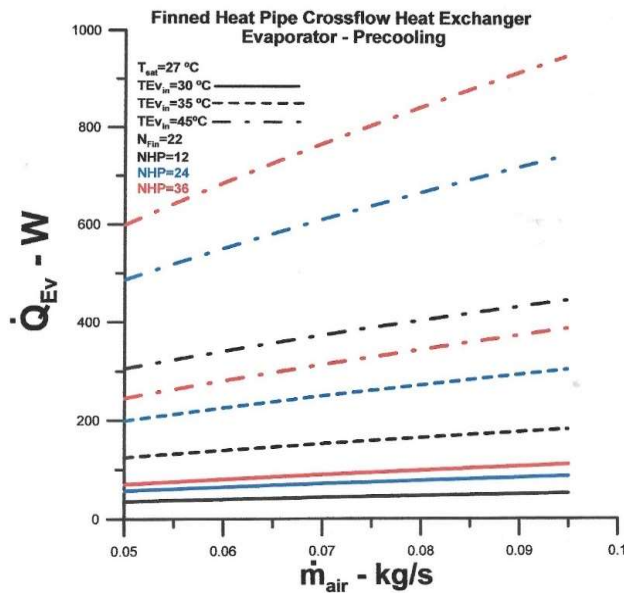

Figure 9. Heat transfer rate at the evaporator versus mass flow rate, number of heat pipes, and air inlet temperature.

Figures 10 and **11** present results for air outlet temperatures in the evaporator region. **Figure 10** emphasizes the influence of the number of heat pipes and air inlet temperature, and **Figure 11** highlights the impact of the number of heat pipes. The air outlet temperature decreases with an increase in the number of heat pipes. On the other hand, the air inlet temperature increases the outlet temperature since the saturation temperature remains constant. The experimental results presented in reference[1] are within the range of theoretically obtained values with similar qualitative trends. The maximum absolute relative error for the evaporator outlet temperature equals 9.9%, and the minor error equals 0.43%.
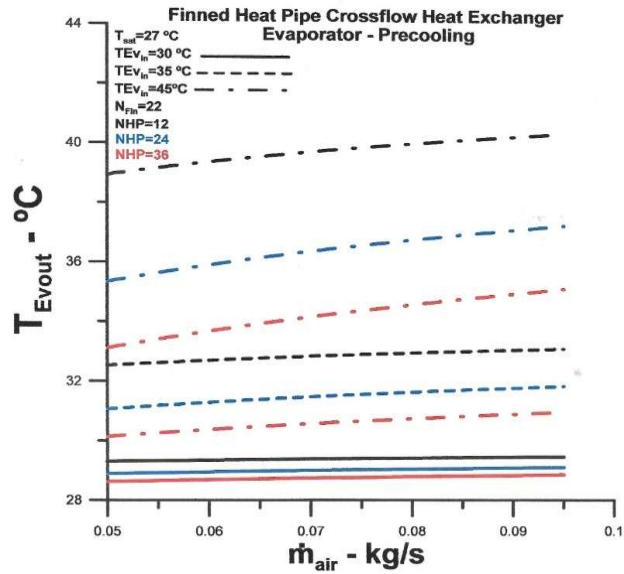
15

Figure 10. Outlet air temperature at the evaporator versus air mass flow rate, number of heat pipes, and air inlet temperature.
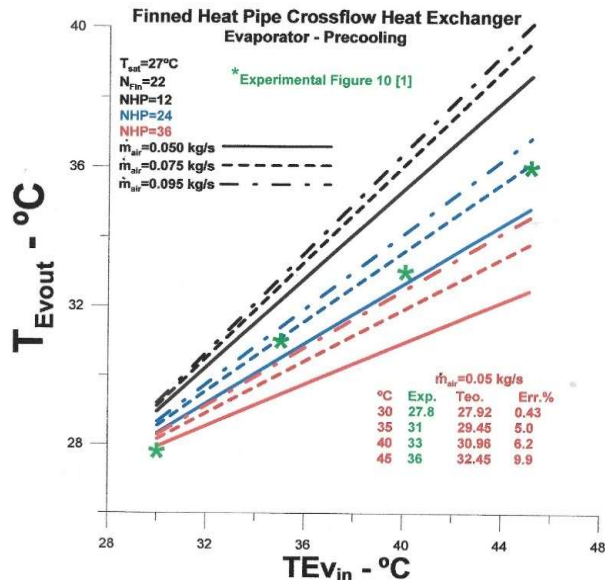

Figure 11. Outlet temperature of the air at the evaporator versus inlet temperature.

The results in **Figures 2–11** demonstrate that the localized theoretical model developed using the concept of thermal efficiency for heat exchangers is consistent in the evaporator region.

The simulations using air inlet temperatures and the number of heat pipes can be used as an instrument for configurations different from those analyzed experimentally. The saturation temperature of 27 °C adopted in the theoretical model proved adequate and consistent with experimental results.

3.2. The condenser section of the heat pipe

Air enters the condenser region at a temperature between 20 °C and 26 °C. As the working fluid condenses, the air is heated and leaves at a higher temperature. The flow rates analyzed are the same for the air in the evaporator, and the fin number equals 25. In this case, the analysis was restricted to the heat transfer rate and outlet temperature, as shown in **Figures 12–15**, because they are the quantities of most significant practical interest.
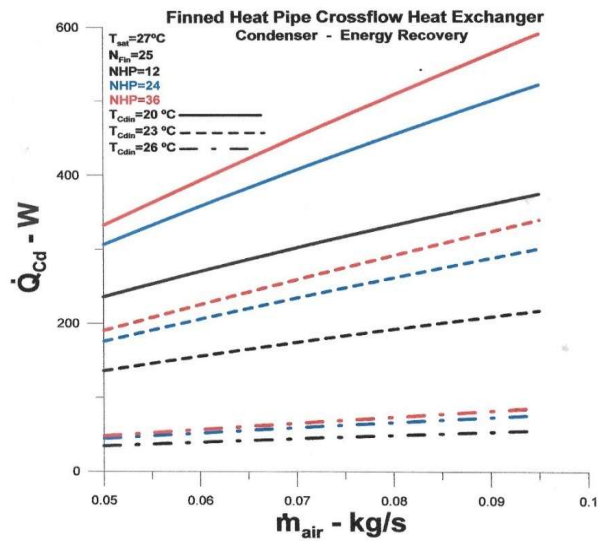
Figure 12. Heat transfer rate at the condenser versus mass flow rate, number of heat pipes, and air inlet temperature.
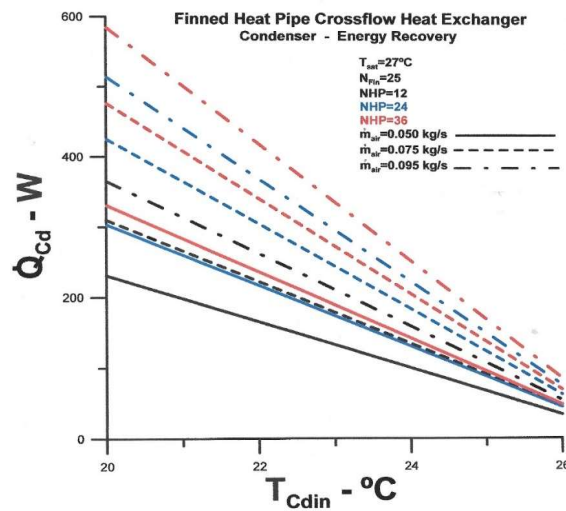
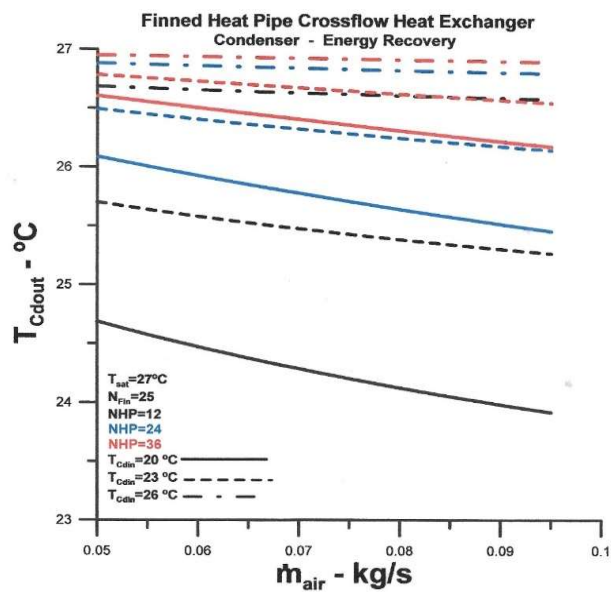**Figure 13.** Heat transfer rate at the condenser versus air inlet temperature.

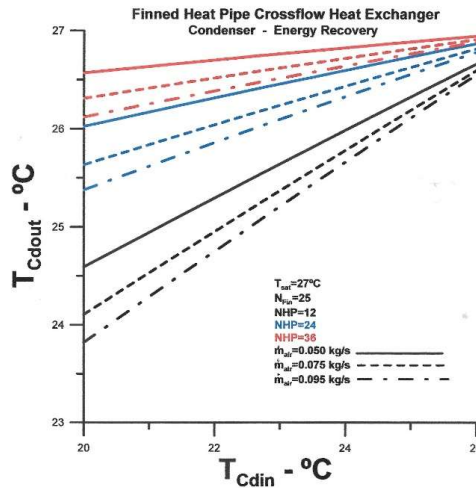**Figure 14.** Outlet air temperature at the condenser versus air mass flow rate.

17

Figure 15. Outlet air temperature at the condenser versus inlet temperature.

Figures 12 and **13** present results for the heat transfer rate as a function of the mass flow rate and the air inlet temperature in the condenser, using the number of heat pipes as parameters. It demonstrates that the influence of the air temperature at the condenser air inlet temperature is significant for larger numbers of heat pipes. The heat transfer rate is higher for lower air inlet temperatures due to the more significant temperature difference between the fluids. Higher flow rates for the air present a higher heat transfer rate between the fluids due to the higher thermal capacity.

The air outlet temperatures in the condenser region, as a function of the inlet temperature, are represented in **Figures 14** and **15**. More significant differences between inlet and outlet temperatures occur for greater numbers of heat pipes. The outlet air temperature is lower for higher air flow rates, as shown in **Figure 15**. The number of heat pipes affects the outlet temperature significantly.

3.3. Finned heat pipe crow-flow heat exchanger (FHPHE)

The overall thermal performance of the heat exchanger is shown in **Figures 16** and **17**. The heat transfer rate associated with the heat exchanger equals the sum of the heat transfer rates obtained for the evaporator and condenser, with the temperature difference between the evaporator inlet temperature and the condenser outlet temperature, as shown in Equations (100) and (101). The global effectiveness is obtained through Equation (102), using the theoretical air outlet temperatures.
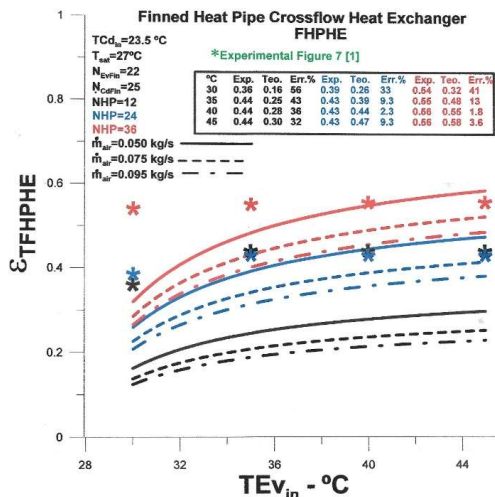

Figure 16. Effectiveness of heat exchanger versus air inlet temperature.
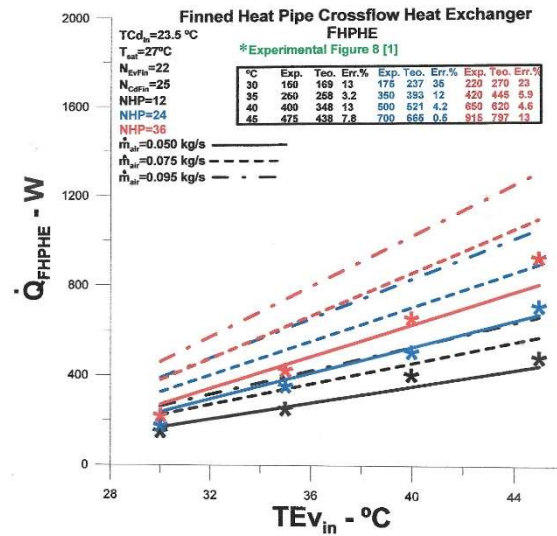
Figure 17. Heat transfer rate of the heat exchanger versus air inlet temperature in the evaporator.

Figure 16 shows the global effectiveness of the heat exchanger as a function of the air inlet temperature in the evaporator. The analysis parameters are the number of heat pipes and air inlet flow rates. Effectiveness increases with increasing air inlet temperature, and the number of heat pipes decreases with increasing flow rate. The experimental results are within the range of theoretically obtained values but show a different qualitative trend. Maximum effectiveness is received for some heat pipes equal to 36 and an inlet temperature equal to 45 °C. The absolute relative error between theoretical and experimental results ranges from 1.8% to 56%.

Figure 17 presents results for the overall heat transfer rate for the heat exchanger under analysis, with airflow variation between 0.050 kg/s and 0.095 kg/s and the inlet temperature of the air in the condenser equal to 23.5 °C. The heat transfer rate increases with airflow and air inlet temperature. However, the most significant effect on the growth of the heat transfer rate is observed in the variation of the inlet air temperature. Compared with experimental results reported in the study of Sukarno et al.[1], the theoretical results show excellent agreement and demonstrate that the model is consistent and can be used for different temperatures within the temperature range covered by the experiment. The maximum relative absolute error obtained for the heat transfer rate is equal to 35%, and the minimum value is equal to 0.5%. It should be noted that the experimental work used to generate theoretical results does not present error analysis.

In summary, it can be said that, although some basic information is not conveyed in the experimental work that serves as a reference, the theoretical model developed covers a wide range of physical situations with a signed agreement and can be applied in similar or more complex cases with the necessary local adjustments. Just as the effectiveness method (ε-NTU) is used as an auxiliary tool in the analysis of experimental designs, the thermal efficiency method, with solid foundations based on the "analogy of fins"[11] and the second law of thermodynamics, is a valuable instrument for localized analysis of heat exchangers. One of the advantages of the thermal efficiency method is that tabulated empirical parameters are usually unnecessary, reducing the difficulty in implementation and increasing the reliability of the results.

4. Conclusion

The thermal performance of a heat exchanger with finned heat tubes used to control the air temperature in the operating room was analyzed. The heat exchanger under analysis uses the evaporator region as an air pre-cooler and the condenser region as energy recovery. Comparisons were made with experimental results and the global theoretical model (ε-NTU). The local and distributed theoretical model used the concept of thermal efficiency for heat exchangers to determine the thermal quantities of interest.

In summary, the main conclusions reached are:

- Using fins improves thermal performance for the heat exchanger configuration under analysis.
- The theoretical results show excellent consistency and demonstrate that the model can be used for different temperatures within the temperature range covered by the experiment. However, the experimental work does not present an error analysis.
- An excellent experimental and theoretical agreement is observed, which proves that the theoretically developed model with local and distributed parameters is consistent and allows advanced global solutions for the air conditioning system analyzed.

Conflict of interest

The author declares no conflict of interest.

Nomenclature

$Asec$	Cross-section area, $[m^2]$
Atr	Heat transfer area, $[m^2]$
Cp	Specific heat, $[\frac{J}{kgK}]$
C	Thermal capacity, $[\frac{W}{K}]$
C_{min}	Minimum thermal capacity, $[\frac{W}{K}]$
$C^* = \frac{C_{min}}{C_{max}}$	
D_h	Hydraulic diameter, $[m]$
Fa	Fin analogy
h	Coefficient of heat convection, $[\frac{W}{m^2K}]$
k	Thermal conductivity, $[\frac{W}{mK}]$
K	Kelvin
kW	Thermal conductivity of the tube, $[\frac{W}{mK}]$
k_{Fin}	Thermal conductivity of the fin, $[\frac{W}{mK}]$
L	Vertical or horizontal length, $[m]$
$\dot{m}_{air}$	Mass flow rate of the air, $[\frac{kg}{s}]$
N_{Fin}	Number of fins
Nu	Nusselt number
Pr	Prandtl number
$\dot{Q}$	Actual heat transfer rate, $[W]$

$\dot{Q}_{max}$	Maximum heat transfer rate, $[W]$
Re	Reynolds number
T	Temperature, $[°C]$
Uo	Global heat transfer coefficient, $[\frac{W}{m^2K}]$

Subscripts

boil	Boiling
Cd	Condenser
Cond	Condenser
effect	Effective
Ev	Evaporator
ext	External
HP	Heat pipe
H	Horizontal
in	Inlet
int	Internal
out	Outlet
sat	Saturation

Greek symbols

α	Thermal diffusivity, $[\frac{m^2}{s}]$
β	The relationship between areas
ρ	Density of the fluid, $[\frac{kg}{m^3}]$
μ	Dynamic viscosity of the fluid, $[\frac{kg}{ms}]$
ν	Kinematic viscosity of the cold fluid, $[\frac{m^2}{s}]$
ε_T	Thermal effectiveness
η_T	Thermal efficiency
ΔT	A difference of temperatures, $[°C]$

Acronyms

FHPHE	Finned heat pipe heat exchanger
Ev	Evaporators
Cd	Condenser
NHP	Number of Heat Pipes
N_{Fin}	Number of Fins
Nrows	Number of rows
NTU	Number of thermal units

Reference

1. Sukarno R, Putra N, Hakim II, et al. Multi-stage heat-pipe heat exchanger for improving energy efficiency of the HVAC system in a hospital operating room. *International Journal of Low-Carbon Technologies* 2021; 16(2): 259–267. doi: 10.1093/ijlct/ctaa048
2. Hakim II, Sukarno R, Putra N. Utilization of U-shaped finned heat pipe heat exchanger in energy-efficient HVAC systems. *Thermal Science and Engineering Progress* 2021; 25: 100984. doi: 10.1016/j.tsep.2021.100984

3.   Putra NSD, Anggoro T, Winarta A. Experimental study of heat pipe heat exchanger in hospital HVAC system for energy conservation. *International Journal of Advance Science Engineering Information Technology* 2017; 7(3): 871–877. doi: 10.18517/ijaseit.7.3.2135

4.   Barrak A. *Heat Pipes Heat Exchanger for HVAC Applications.* IntechOpen; 2021.

5.   Stewart SW, Shelton SV, Aspelund KA. Finned tube heat exchanger optimization methodology. In: Proceedings of the 2nd International Conference on Heat Transfer, Fluid Mechanics and Thermodynamics; 23–26 June 2003, Victoria Falls, Zambia.

6.   Nogueira E. Thermo-hydraulic optimization of shell and externally finned tubes heat exchanger by the thermal efficiency method and second law of thermodynamics. *International Journal of Chemical and Process Engineering Research* 2022; 9(1): 21–41. doi: 10.18488/65.v9i1.3130

7.   Górecki G, Łęcki M, Gutkowski AN, et al. Experimental and numerical study of heat pipe heat exchanger with individually finned heat pipes. *Energies* 2021; 14(17): 5317. doi: 10.3390/en14175317

8.   Jouhara H, Chauhan A, Nannou T, et al. Heat pipe based systems—Advances and applications. *Energy* 2017; 128: 729–754. doi: 10.1016/j.energy.2017.04.028

9.   Jouhara H, Almahmoud S, Brough D, et al. Experimental and theoretical investigation of the performance of an air to water multi-pass heat pipe-based heat exchanger. *Energy* 2021; 219: 119624. doi: 10.1016/j.energy.2020.119624

10.   Rohsenow WM. A method of correlating heat transfer data for surface boiling of liquids. *Transactions of the American Society of Mechanical Engineers* 1952; 74(6): 969–975. doi: 10.1115/1.4015984

11.   Fakheri A. Heat exchanger efficiency. *AMSE Journal of Heat and Mass Transfer* 2007; 129(9): 1268–1276. doi: 10.1115/1.2739620

12.   Nogueira É. Thermal performance in heat exchangers by the irreversibility, effectiveness, and efficiency concepts using nanofluids. *Journal of Engineering Sciences* 2020; 7(2): F1–F7. doi: 10.21272/jes.2020.7(2).f1